THE COUPLING OF DIFFUSION, REACTION AND MECHANICS IN BIOLOGICAL GROWTH: THEORY AND NUMERICAL MODELS

DRAFT

19^{th} September, 2005

Abstract

Growth in biological tissue depends upon cascades of complex biochemical reactions involving several species, as well as their transport through the extra cellular matrix and diffusion across cell membranes. In this work, a theoretical and numerical framework for the macroscopic treatment of growth is formulated within the context of open system continuum thermodynamics. Assumptions central to classical mechanics being too restrictive to capture such detail, this treatment involves the introduction of additional quantities (including mass sources/sinks, mass fluxes, terms for energy and momentum transfer between species) and deduces implications for balance laws. The framework, consistent with classical mixture theory, accounts for the multiple inter-converting and interacting species present in the tissue. Systematic adherence to fundamental physical principles, such as frame indifference of the response in the reference configuration and non-violation of the dissipation inequality, result in constitutive laws whose forms are clearly motivated and arise naturally from the treatment. Notably, the transport of the extra cellular fluid relative to the matrix is shown to be driven by the gradients of stress, concentration and chemical potential—a coupling of mass transport and mechanics that emerges directly.

A finite element formulation employing a staggered scheme is implemented to solve the coupled partial differential equations that arise from the theory. Nonlinear projection methods are utilised to handle incompressibility, mixed methods for stress-gradient driven fluxes and energy-momentum conserving algorithms are used for dynamics. Our current tissue of interest being engineered *in vitro* tendon, the numerical examples are in this context. The examples serve to demonstrate aspects of the coupled phenomena as the tissue grows. The classes of initial and boundary conditions imposed, and model geometry match parallel experiments (which form another integral part of a larger project studying growth and remodelling of engineered tissues). Representatively, concentration or flux boundary conditions (tissue exposed to fluid in a bath, fluid injected in at the boundary) are imposed for the balance of mass governing the fluid phase. Conditions in an experiment being consistent with specification of quantities in the current configuration, noteworthy differences that arise when solving these equations in terms of quantities in this configuration, as opposed to the reference configuration, where the equations are initially developed, are accentuated.

During the course of applying the theory to our system of interest, various meaningful modelling choices are made to tailor it to be representative of tendon constructs. While this tends to hint at a loss of generality, it is important to recognise that the fundamental theory and physical principles employed are still applicable to a larger class of problems, both from biology (injury mechanisms, wound healing, scarring and surgical repair, ...) as well as from other diverse fields (from porous soil mechanics, to diffusion of air through anisotropic rubber materials in automobile tyres). With further refinements to the theory and concurrent maturation of the resulting computational framework, it is of future interest to extend the application of the theory to other classes of problems.

Contents

Chapter 1

Introduction

1.1 Specific goals

The fundamental objectives of this research project are as follows:

- Formulate a sufficiently general and detailed continuum field theory for macroscopic growth, which includes a complete treatment of mass transport coupled with mechanics, and implement a demonstrative numerical scheme.
- Make systematic and physiologically relevant modelling choices to tailor this general formulation to better represent our current tissue of interest, engineered tendon constructs, and use it to model and predict the response of the same.

1.2 Background and motivation

The processes involved in the development of biological tissue, though numerous and involving several cascades of complex interactions, are generally broken down into the distinct processes of *growth*, *remodelling*, and *morphogenesis* in biomechanics literature [Taber, 1995]. This present work treats these processes as mathematically independent and its focus, growth, is defined to be an addition[1] of mass through the processes of mass transport and biochemical reactions. Additionally, this is a continuum treatment at a macroscopic scale, rather than at a cellular or sub-cellular level.

Recognising the complexity of the system presented (that it is open with respect to mass and energy, and contains numerous species which are capable of interacting and inter-converting) and the limitations of classical mechanics, additional terms (scalar mass sources/sinks, vectorial mass fluxes and terms for momentum and energy transfer between species) are introduced enhancing classical balance laws. The complex cascades of bio-

[1] Or depletion, if one is dealing with the converse process of *resorption*.

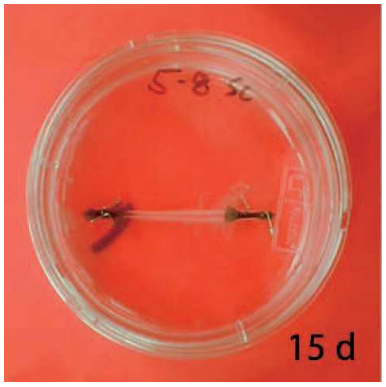

Figure 1.1: Engineered tendon constructs [Calve et al., 2004].

chemical reactions are treated in an elementary fashion, using source-sink terms to govern inter-conversion and mass fluxes that supply nutrient and remove byproducts.

In the context of biological growth, the notion of a mass source was first introduced in [Cowin and Hegedus, 1976]. The notion of a mass flux is a more recent introduction [Epstein and Maugin, 2000], but this work regarded fluxes purely as irreversible fluxes of momentum and entropy. In [Kuhl and Steinmann, 2003], configurational forces motivate mass flux where the transported species is the same material as the tissue itself. These few cited examples of previous work are just a subset of a large body of theoretical and computational literature in this area. But, while the details vary, the body of literature represented by these works is largely based upon a single species undergoing transport and being produced/annihilated.

In addition to the possibility of multiple species undergoing cascades of reactions, the full range of driving forces for mass transport, such as chemical potential gradients, stress gradients, external body forces such as gravity, has not been systematically treated previously. Most previous coupling between transport and mechanics has been through growth-induced residual stress, as described in Section 2.1.4. As indicated at the outset, this work is aimed at a complete treatment mass transport, coupled with mechanics, for the growth problem.

Though the formulation is applicable to a large class of open systems with multiple species potentially participating in reactions, here it is used to model and predict the response and evolution of one specific tissue of interest to us, our engineered tendon constructs. These are functionally immature tendons formed by the self assembly of tendon fibroblasts *in vitro* [Calve et al., 2004]. Figure 1.1 shows a sample construct 15 days after it has been plated. During the course of development of this tissue, it undergoes numerous complex processes, but for the purposes of this growth model, we are focused on the evolution of concentrations of substances such as collagen (see Figure 1.2), as well as their dependence on mechanics.

There are compelling clinical reasons to study tendons. Tendons consist mostly of collagen and perhaps provide the simplest physiologically relevant setting to understand the chemical and mechanical factors affecting proper collagen deposition. Collagen is the most important structural component of soft biotissue. Errors in collagen deposition cause important types of tissue dysfunction ranging from *cardiomyopathy* (hypertrophy of collagen

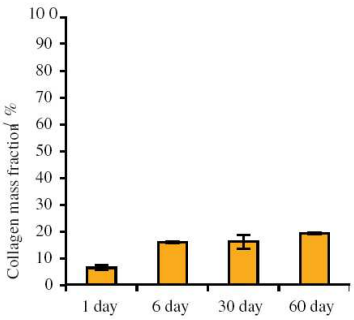

Figure 1.2: The evolution of collagen concentration with age [Calve et al.].

makes the heart too stiff to undergo proper volumetric change) to *hypertrophic scarring* in burns (where the morphology of collagen is whirled rather than aligned in overly stiff scars).

Additionally, there are a large number of musculoskelital injuries each year which result in damage to soft tissues, including tendon. For tendons damaged beyond repair, replacement is necessary. This replacement must incorporate most native properties of tendon to restore function. However, such transplantation is limited by the availability of viable autograft, resulting in the use of synthetic materials which are unable to restore long term function due to incompatibility. Thus, a need exists for replacements which incorporate as many native properties as possible, necessitating a systematic study of engineered tendon.

Chapter 2

Preliminary Work

2.1 Mathematical formulation of growth

In the following sections, the basic dynamical equations of the continuum formulation developed from physical principles governing the behaviour of growing tissue are summarised[1]. Section 2.1.1 helps define the system and introduces fundamental quantities characterising it. Sections 2.1.2 and 2.1.3 present the balance of mass and balance of momenta respectively. Section 2.1.4 describes the treatment of growth kinematics. Key concepts from thermodynamics, the conservation of energy and the entropy inequality, are the subject of Section 2.1.5. Finally, the functional forms of the constitutive relations derived from the Clausius-Duhem inequality are highlighted in Section 2.1.6.

2.1.1 Defining the system

The tissue of interest is an open subset of $\mathbb{R}^3$ with a piecewise smooth boundary. At a reference placement of the tissue, Ω_0, points in the tissue are identified by their reference positions, $\boldsymbol{X} \in \Omega_0$. The motion of the tissue is a sufficiently smooth bijective map $\boldsymbol{\varphi} : \overline{\Omega}_0 \times [0,T] \to \mathbb{R}^3$, where $\overline{\Omega}_0 := \Omega_0 \cup \partial\Omega_0$. At a typical time $t \in [0,T]$, $\boldsymbol{\varphi}(\boldsymbol{X},t)$ maps a point $\boldsymbol{X}$ to its current position, $\boldsymbol{x}$. In its current configuration, the tissue occupies a region $\Omega_t = \boldsymbol{\varphi}_t(\Omega_0)$. These details are symbolised in Figure 2.1. The deformation gradient $\boldsymbol{F} := \mathrm{GRAD}[\boldsymbol{\varphi}]$ is the tangent map of $\boldsymbol{\varphi}$ (where $\mathrm{GRAD}[\bullet]$ is the gradient operator in the reference configuration).

The tissue consists of numerous species, each designated as part of a certain representative class—a *solid* phase, consisting of solid collagen fibrils, proteoglycans and cells, denoted by c, a *fluid* phase denoted by f and typified by water bound loosely to proteoglycans, or a *solute* phase, consisting of precursors to reactions, byproducts, nutrients, and other regulatory chemicals, denoted by s. In what follows, an arbitrary species will be denoted by ι.

The fundamental quantities of interest are mass concentrations of a species (the mass of

[1]Detailed derivations of the same can be obtained from [Garikipati et al., 2004].

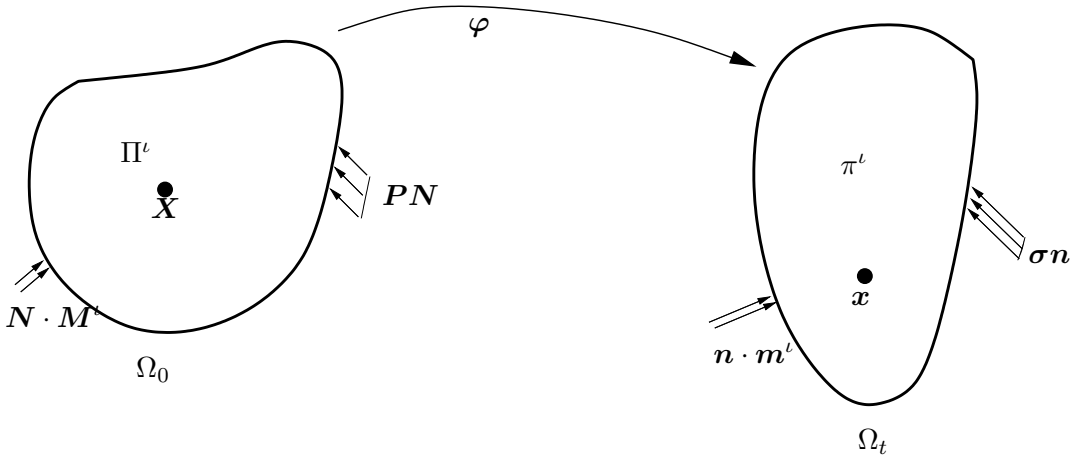

Figure 2.1: The continuum tissue with growing and diffusing species under stress.

the species per unit reference system volume), $\rho_0^\iota(\boldsymbol{X}, t)$. Formally, these quantities can also be thought of in terms of the maps $\rho_0^\iota : \overline{\Omega}_0 \times [0, T] \to \mathbb{R}$. The formulation imposes some smoothness requirements on the distributions of these concentrations. By definition, the total material density of the tissue at a point is a sum of these concentrations over all species $\sum_\iota \rho_0^\iota = \rho_0$. Other than the solid phase, s, all phases have mass fluxes, $\boldsymbol{M}^\iota$. These are mass flow rates per unit cross-sectional area in the reference configuration *defined relative to the solid phase*. Except for the fluid phase, f, all phases have suitable mass sources/sinks, Π^ι, suitably encapsulating the complexity of the biochemistry.

2.1.2 Balance of mass for an open system

As a result of mass transport and inter-conversion of species introduced previously, the concentrations, ρ_0^ι, change with time. In local form, the balance of mass for an arbitrary species in the reference configuration is

$$\frac{\partial \rho_0^\iota}{\partial t} = \Pi^\iota - \mathrm{DIV}[\boldsymbol{M}^\iota], \ \forall\, \iota, \tag{2.1}$$

recalling that, in particular, $\boldsymbol{M}^s = \boldsymbol{0}$ and $\Pi^f = 0$. Here, $\mathrm{DIV}[\bullet]$ represents the divergence operator in the reference configuration. The functional forms of Π^ι are chosen to represent the biochemistry (which, for e.g., could additionally include the dependence of the rate of tissue formation on the state of local stress, as in [Harrigan and Hamilton, 1993]) and the fluxes, $\boldsymbol{M}^\iota$, are determined from the thermodynamically motivated constitutive relations described in Section 2.1.6.

The behaviour of the entire system can be determined by summing Eq. (2.1) over all species ι. Additionally, sources/sinks satisfy the relation

$$\sum_\iota \Pi^\iota = 0, \tag{2.2}$$

which is consistent with the Law of Mass Action for reaction rates and with mixture theory [Truesdell and Noll, 1965].

Though it is not mathematically infeasible to solve the problem in terms of Eq. (2.1) written out for the various species, it is important to note that soft tissues are capable of undergoing considerable deformation. The current domain of the physical system, Ω_t, and its boundary, change in time. In order to apply boundary conditions (either specification of species flux or concentration) that are physical, it is straightforward to use the local form of the balance of mass in the current configuration,

$$\frac{\mathrm{d}\rho^\iota}{\mathrm{d}t} = \pi^\iota - \mathrm{div}[\boldsymbol{m}^\iota] - \rho^\iota \mathrm{div}[\boldsymbol{v}], \ \forall\, \iota, \tag{2.3}$$

where $\rho^\iota(\boldsymbol{x}, t)$, $\pi^\iota(\boldsymbol{x}, t)$, and $\boldsymbol{m}^\iota(\boldsymbol{x}, t)$ are the current mass concentration, source and mass flux of species ι respectively. $\mathrm{div}[\bullet]$ is the spatial divergence operator, and the time derivative on the left hand-side in Eq. (2.3) is the material time derivative, that may be written explicitly as $\frac{\partial}{\partial t}|_X$, implying that the reference position is held fixed.

Again, it must be emphasised that only the final forms of the equations are presented here as a summary. Detailed derivations of the same are available in an earlier work [Garikipati et al., 2004]. Additionally, in the interest of clarity, the descriptions in the subsequent sections are entirely in terms of quantities in the reference configuration.

2.1.3 Balance of momenta

In real tissues, the terms that appear on the right hand-side in Eq. (2.1), the species production rate and flux, are strongly dependent on the local state of stress. To correctly model this coupling, the balance of linear momentum should be solved to determine the local state of strain and stress.

As outlined in Section 2.1.1, the deformation of the tissue is characterised by the map $\boldsymbol{\varphi}(\boldsymbol{X}, t)$. Recognising that the deposited solid collagen fibrils do not undergo mass transport, the formulation uses the material velocity of this phase, defined by the relation $\boldsymbol{V} = \partial\boldsymbol{\varphi}/\partial t$, as a primitive variable for mechanics. The motion of the remaining species are split into a deformation along with this solid phase, and mass transport relative to it. To this end, analogous to $\boldsymbol{M}^\iota$ in the balance of mass, it is useful to define the material velocity of a species ι *relative to the solid skeleton* as: $\boldsymbol{V}^\iota = (1/\rho_0^\iota)\boldsymbol{F}\boldsymbol{M}^\iota$. Thus, the total material velocity of a phase ι is $\boldsymbol{V} + \boldsymbol{V}^\iota$. Due to existence of multiple species, the total first Piola-Kirchhoff stress tensor $\boldsymbol{P}$ is obtained by summing the partial stresses $\boldsymbol{P}^\iota$ (borne by a species ι) over all the species present[2]. With the introduction of these additional quantities, the balance of linear momentum in local form for a species ι in Ω_0 is

$$\rho_0^\iota \frac{\partial}{\partial t}\left(\boldsymbol{V} + \boldsymbol{V}^\iota\right) = \rho_0^\iota\left(\boldsymbol{g} + \boldsymbol{q}^\iota\right) + \mathrm{DIV}[\boldsymbol{P}^\iota] - \left(\mathrm{GRAD}\left[\boldsymbol{V} + \boldsymbol{V}^\iota\right]\right)\boldsymbol{M}^\iota, \tag{2.4}$$

[2]In reality, the amino acids, nutrients and regulators are in solution under low relative concentrations. They do not bear any appreciable stress.

where $\boldsymbol{g}$ is the body force per unit mass, and $\boldsymbol{q}^\iota$ is an interaction term denoting the force per unit mass exerted upon ι by all other species present. The final term with the gradient denotes the contribution of the flux to the balance of momentum. In practise, the relative magnitude of the fluid mobility (and hence flux) is small, so the final term on the right hand side of Eq. (2.4) is negligible, resulting in a more classical form of the balance of momentum.

The behaviour of the entire tissue is obtained by summing Eq. (2.4) over all the species present. Additionally, recognising that the rate of change of momentum of the entire tissue is affected only by external agents and is independent of internal interactions, the following relation arises.

$$\sum_i \left(\rho_0^\iota \boldsymbol{q}^\iota + \Pi^\iota \boldsymbol{V}^\iota\right) = 0. \tag{2.5}$$

This is also consistent with classical mixture theory [Truesdell and Noll, 1965].

The balance of angular momentum in this formulation results in a symmetric Cauchy stress tensor, $\boldsymbol{\sigma} = \boldsymbol{\sigma}^{\mathrm{T}}$, mirroring the result obtained in classical continuum mechanics. This is in contrast to the non-symmetric Cauchy stress arrived at in [Epstein and Maugin, 2000]. This difference appears to stem from their use of $\boldsymbol{V} = \partial\boldsymbol{\varphi}/\partial t$ as the material velocity of a single species, rather than multiple species with material velocities $\boldsymbol{V} + \boldsymbol{V}^\iota$.

2.1.4 Kinematics: The elasto-growth decomposition

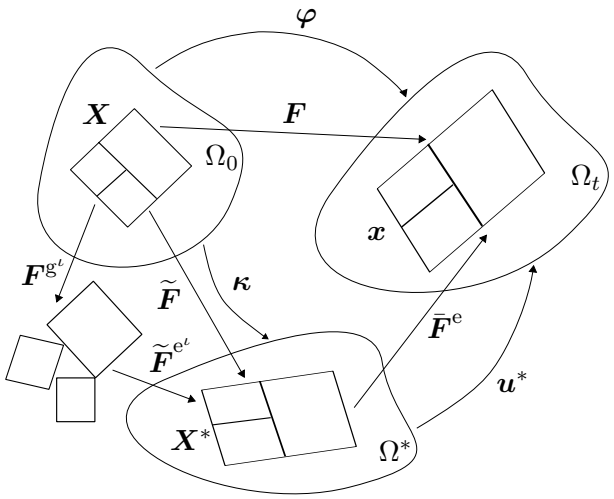

Figure 2.2: The kinematics of growth.

Local volumetric changes are associated with changes in the concentrations of species. The material of the species swells with an increase in concentration, and shrinks as its concentration decreases. Additional coupling between mass transport and mechanics stems from this phenomena. This work's treatment of the finite strain kinematics involves a decomposition of the deformation gradient into a geometrically necessitated elastic deformation

accompanying growth, and an additional elastic deformation due to external stress. This split is analogous to the classical decomposition of multiplicative plasticity [Lee, 1969] and is similar to the approach followed in existing literature on biological growth (see, for e.g., [Taber and Humphrey, 2001, Ambrosi and Mollica, 2002]).

The split itself is visualised in Figure 2.2. Assuming that the volume changes associated with growth described above are isotropic, a simple form for the *growth deformation gradient tensor* is $\boldsymbol{F}^{\mathrm{g}^\iota} = \frac{\rho_0^\iota}{\rho_{0_{\mathrm{ini}}}^\iota}\mathbf{1}$, where $\rho_{0_{\mathrm{ini}}}^\iota(\boldsymbol{X})$ can be interpreted as an original reference state where the species would be stress free in the absence of a deformation, and $\mathbf{1}$ is the identity tensor. Additionally, this being a local definition, the action of $\boldsymbol{F}^{\mathrm{g}^\iota}$ alone can result in incompatibility. To ensure compatibility, there is a further elastic deformation $\widetilde{\boldsymbol{F}}^{\mathrm{e}^\iota}$. Thus, the total deformation gradient $\boldsymbol{F} = \bar{\boldsymbol{F}}^{\mathrm{e}}\widetilde{\boldsymbol{F}}^{\mathrm{e}^\iota}\boldsymbol{F}^{\mathrm{g}^\iota}$, and internal stresses in the tissue arise due to the compatibility restoring tensor $\widetilde{\boldsymbol{F}}^{\mathrm{e}^\iota}$.

2.1.5 Thermodynamics: Balance of energy and the entropy inequality

In addition to the terms defined previously, we define the internal energy per unit mass of species ι, denoted e^ι; the heat supply to species ι per unit reference volume, r_0^ι; and the partial heat flux vector of ι, $\boldsymbol{Q}^\iota$ on Ω_0. Since there are numerous species present, an interaction term $\tilde{e}^\iota$, which accounts for the internal energy transferred to ι by all other species, is also defined. With these quantities defined, the local form of the balance of energy for an arbitrary species ι is

$$\rho_0^\iota \frac{\partial e^\iota}{\partial t} = \boldsymbol{P}^\iota : \mathrm{GRAD}\left[\boldsymbol{V} + \boldsymbol{V}^\iota\right] - \mathrm{DIV}\left[\boldsymbol{Q}^\iota\right] + \rho_0^\iota r^\iota + \rho_0^\iota \tilde{e}^\iota - \mathrm{GRAD}\left[e^\iota\right] \cdot \boldsymbol{M}^\iota. \tag{2.6}$$

As before, the behaviour of the entire tissue is obtained by summing Eq. (2.6) over all ι and this also results in another relation relating the interaction energies to the interaction forces, sources and relative velocities, identical to what is obtained in mixture theory.

Let η^ι be the entropy per unit mass of species ι, and θ the absolute temperature. The entropy inequality holds for the system as a whole, and has the following form.

$$\sum_\iota \rho_0^\iota \frac{\partial \eta^\iota}{\partial t} \geq \sum_\iota \left(\frac{\rho_0^\iota r^\iota}{\theta} - \mathrm{GRAD}\left[\eta^\iota\right] \cdot \boldsymbol{M}^\iota - \frac{\mathrm{DIV}\left[\boldsymbol{Q}^\iota\right]}{\theta} + \frac{\mathrm{GRAD}\left[\theta\right] \cdot \boldsymbol{Q}^\iota}{\theta^2} \right). \tag{2.7}$$

2.1.6 Functional forms of the constitutive relations

As is customary in field theories of continuum physics, we first obtain the Clausius-Duhem inequality by multiplying Eq. (2.7) by the temperature θ and subtracting it from Eq. (2.6). Then, the internal energy of a species ι is assumed to be of a sufficiently general form: $e^\iota = \hat{e}^\iota(\boldsymbol{F}^{\mathrm{e}^\iota}, \eta_0^\iota, \rho_0^\iota)$. Substituting this in the Clausius-Duhem inequality and applying the

chain rule results in an inequality later specified constitutive relations *must* not violate. Only the valid constitutive laws relevant to the examples that follow are listed here. For details, see [Garikipati et al., 2004].

Most notably, the fluid flux relative to the collagen takes the form

$$\boldsymbol{M}^f = \boldsymbol{D}^f \left(\rho_0^f \boldsymbol{F}^T \boldsymbol{g} + \boldsymbol{F}^T \mathrm{DIV}\left[\boldsymbol{P}^f\right] - \mathrm{GRAD}\left[e^f - \theta\eta^f\right] \right), \tag{2.8}$$

where $\boldsymbol{D}^f$ is the positive semidefinite mobility of the fluid and the temperature field is assumed isothermal for physiological correctness. The terms in the parenthesis on the right hand-side sum up to give the total driving force for transport. The first term is the contribution due to gravitational acceleration. The second term arises from stress divergence. For instance, fluid tends to move down a compressive pressure gradient. The third term can be thought of as the gradient of a chemical potential. The included entropy gradient in this term results in classical Fickean diffusion if only mixing entropy exists.

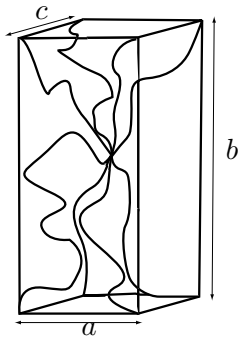

Figure 2.3: Worm like chains assembled into an anisotropic eight-chain model.

A constitutive form for the partial stress of a species ι allowable by the Second Law of Thermodynamics is that of a hyperelastic material: $\boldsymbol{P}^\iota = \rho_0^\iota \frac{\partial e^\iota}{\partial \boldsymbol{F}^{\mathrm{e}^\iota}} \boldsymbol{F}^{\mathrm{g}^\iota - T}$. The fluid phase is modelled as ideal and nearly incompressible which results in a stored energy function of the form: $\rho^f \hat{e}^f = \frac{1}{2}\kappa(\det(\boldsymbol{F}^{\mathrm{e}^f}) - \mathbf{1})^2$. For the collagen phase, the continuum stored energy function e^c is based on the worm-like chain model. The model has been described and implemented into an anisotropic representative volume element in [Bischoff et al., 2002]. In summary, the strain energy density of a single constituent chain (see Figure 2.3) of the eight-chain model is,

$$\begin{aligned} \widetilde{\rho_0}^{\mathrm{c}} \hat{e}^{\mathrm{c}}(\boldsymbol{F}^{\mathrm{e}^{\mathrm{c}}}, \rho_0^{\mathrm{c}}) &= \frac{Nk\theta}{4A}\left(\frac{r^2}{2L} + \frac{L}{4(1-r/L)} - \frac{r}{4}\right) \\ &- \frac{Nk\theta}{4\sqrt{2L/A}}\left(\sqrt{\frac{2A}{L}} + \frac{1}{4(1-\sqrt{2A/L})} - \frac{1}{4}\right)\log(\lambda_1^{a^2}\lambda_2^{b^2}\lambda_3^{c^2}) \\ &+ \frac{\gamma}{\beta}(J^{\mathrm{e}^\iota - 2\beta} - 1) + 2\gamma\mathbf{1}\colon \boldsymbol{E}^{\mathrm{e}^{\mathrm{c}}} \end{aligned} \tag{2.9}$$

,

where N is the chain density, k is Boltzmann's constant, r is the end-to-end length of a chain, L is the fully extended length and A is the persistence length which measures the degree to which the curve departs from a straight line. The preferred orientation of the tendon collagen is described by the anisotropic unit cell with sides a, b and c (as in Figure 2.3). The elastic stretches along the unit cell axes are denoted by λ_1, λ_2, λ_3 and $\boldsymbol{E}^{\mathrm{e}^{\mathrm{c}}}$ is the elastic Lagrange strain of collagen. The factors β and γ control bulk compressibility. The end to end lengths are given by $r = \frac{1}{2}\sqrt{a^2\lambda_1^{\mathrm{e}^2} + b^2\lambda_2^{\mathrm{e}^2} + c^2\lambda_3^{\mathrm{e}^2}}$, and $\lambda_I^{\mathrm{e}} = \sqrt{\boldsymbol{N}_I \cdot \boldsymbol{C}^{\mathrm{e}}\boldsymbol{N}_I}$.

2.2 Numerical implementation

2.2.1 A brief look at the computational formulation

The theory presented in the preceding sections results in nonlinear coupled partial differential equations that need to be solved. A finite element formulation employing a staggered scheme based upon operator splits [Armero, 1999, Garikipati and Rao, 2001] has been implemented in `FEAP` [Taylor, 1999] to solve the coupled problem. The basic solution scheme involves keeping one of the fields, say the displacement field, fixed while solving for the other, the mass transport problem in this instance. The resulting concentration field is then fixed to solve the mechanics problem. This procedure is repeated until the resulting fields satisfy the differential equations within some suitable tolerance.

The transient solution is obtained for mechanics using energy-conserving schemes as detailed in [Simo and Tarnow, 1992]. Backward Euler is used as the time-stepping algorithm for mass transport. Nonlinear projection methods [Simo et al., 1985] are used to treat the near-incompressibility imposed by water. Mixed methods [Garikipati and Rao, 2001] are used for stress/strain gradient driven fluxes.

2.2.2 Numerical example

The following example aims to demonstrate the mathematical formulation and aspects of the coupled phenomena as the tissue grows. The model geometry, based on the engineered tendon constructs (see Figure 1.1), is a cylinder 12 mm in length and 1 mm^2 in cross-sectional area. Only two phases—fluid and collagen—are included for the mass transport and mechanics. The collagen is represented by the anisotropic worm-like chain model outlined previously (see Section 2.1.6) and the fluid phase is modelled as ideal and nearly incompressible. The parameters used in the analysis are as presented in Table 2.1. The values chosen are representative of the kinds of biological systems we are working with. The classes of initial and boundary conditions imposed are also based on physical experiments.

Since we only have two species and we want to demonstrate growth, an "artificial" fluid sink Π^{f} is introduced following simple first order kinetics. The collagen source will be the negative of the fluid sink: $\Pi^{\mathrm{f}} = -k^{\mathrm{f}}(\rho_0^{\mathrm{f}} - \rho_{0_{\mathrm{ini}}}^{\mathrm{f}})$; $\Pi^{\mathrm{c}} = -\Pi^{\mathrm{f}}$, where k^{f} is the reaction rate, and $\rho_{0_{\mathrm{ini}}}^{\mathrm{f}}$ is the initial concentration of fluid. When $\rho_0^{\mathrm{f}} > \rho_{0_{\mathrm{ini}}}^{\mathrm{f}}$, this acts as a source for collagen.

Parameter	Symbol	Value	Units
Chain density	N	7×10^{21}	m^{-3}
Temperature	θ	310.0	K
Persistence length	A	1.3775	–
Fully-stretched length	L	25.277	–
Unit cell axes	$a,\ b,\ c$	9.3, 12.4, 6.2	–
Bulk compressibility factors	$\gamma,\ \beta$	1000, 4.5	–
Fluid bulk modulus	κ	1	GPa
Fluid mobility tensor	$D_{ij} = D\delta_{ij}$	1×10^{-8}	$\mathrm{m}^{-2}\mathrm{sec}$
Fluid conversion reac. rate	k^{f}	$-1. \times 10^{-7}$	sec^{-1}
Gravitational acceleration	$\boldsymbol{g}$	9.81	$\mathrm{m.sec}^{-2}$
Fluid mol. wt.	$\mathcal{M}^{\mathrm{f}}$	2.9885×10^{-23}	kg

Table 2.1: Material parameters used in the analysis.

The mixing entropy of fluid in the mixture with collagen is written as $\eta^f_{\mathrm{mix}} = -\frac{k}{\mathcal{M}^{\mathrm{f}}}\log(\frac{\rho^{\mathrm{f}}_0}{\rho_0})$, where $\mathcal{M}^{\mathrm{f}}$ is the molecular weight of the fluid.

The boundary conditions simply corresponding to immersing the tendon in a nutrient rich bath. The initial collagen concentration is 500 $\mathrm{kg/m}^3$ everywhere and the fluid concentration is 400 $\mathrm{kg/m}^3$ everywhere. This is exposed to a bath where the fluid concentration is 500 $\mathrm{kg/m}^3$, so with these concentration boundary conditions set, nutrient rich fluid rushes into the tissue, and growth occurs to form more collagen. The following plots present a few results from the analysis.

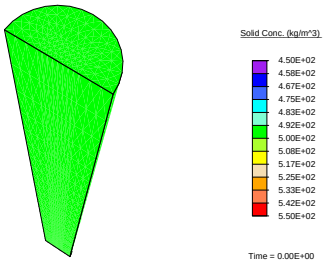

Figure 2.4: The collagen concentration ($\mathrm{kg/m}^3$) initially.

Figure 2.4 shows the initial collagen concentration in the tendon. After it has been immersed in a nutrient rich bath for half an hour, the tendon has grown and the collagen concentration is now higher as seen in Figure 2.5. On performing a simple uniaxial tension test on the tendon before and after growth, it is observed that the grown tissue is stiffer and stronger as seen in Figure 2.6. Additionally, the swelling of the tendon as it is immersed in the bath takes place in two clear regimes as seen in Figure 2.7. There as an initial rapid swelling in a diffusion dominated regime, and a slower growth dominated swelling later on.

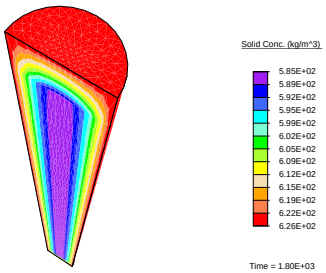

Figure 2.5: The collagen concentration (kg/m^3) after 1800 seconds.

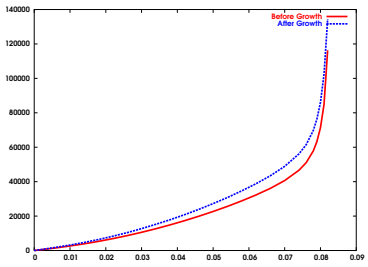

Figure 2.6: The stress (Pa) vs extension (m) curves before and after growth.

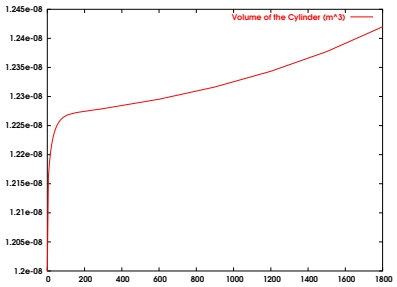

Figure 2.7: The volume of the tendon (m^3) evolving with time.

Chapter 3

Proposed Plan of Advancement

The following sections provide an abbreviated look at future directions we propose the current framework and resulting numerical implementation evolve. Since each of these areas provide extensive scope for development, the following exposition will keep returning to a common theme—better represent the biochemistry—which also aids to relate these different areas.

3.1 Revisiting modelling choices

As has been described previously, growth in biological tissue depends upon cascades of complex biochemical reactions involving several species. In the numerical example described in Section 2.2.2, a simple first order rate law was used to define the collagen source term. In order to better represent the biochemistry, it is appropriate to use more sophisticated forms for the source. It is proposed that a few reasonable choices be implemented and the degree to which the simulations reflect experiments be examined.

Two promising forms include *enzyme kinetics* [Michaelis and Menten, 1913],

$$\Pi^{\mathrm{s}} = \frac{(\Pi^{\mathrm{s}}_{\max}\rho^{\mathrm{s}})}{(\rho^{\mathrm{s}}_{m} + \rho^{\mathrm{s}})}\rho_{\mathrm{cell}}, \quad \Pi^{\mathrm{c}} = -\Pi^{\mathrm{s}}, \tag{3.1}$$

where s stands for a solute phase, ρ_{cell} is the cell concentration and $\rho^{\mathrm{s}}_{m} = \frac{(k_2+k_{-1})}{k_1}$, where k_1, k_{-1} and k_2 are the rates of the following $\mathrm{E} + \mathrm{S} \underset{k_{-1}}{\overset{k_1}{\rightleftharpoons}} \mathrm{ES} \xrightarrow{k_2} \mathrm{E} + \mathrm{P}$ involving enzymes, substrates and products, and *strain energy dependent* forms weighted by relative densities [Harrigan and Hamilton, 1993],

$$\Pi^{\mathrm{c}} = (\frac{\rho^{\mathrm{c}}_{0}}{\rho^{\mathrm{c}}_{0_{\mathrm{ini}}}})^{-m}\Psi_0 - \Psi^{*}_{0}, \tag{3.2}$$

where Ψ^{*}_{0} represents a basal value of the energy density.

These sorts of modelling choices were also made in other areas, for e.g., the selection of a constitutive model for collagen stress based on a strain energy derived from the worm-like

chain model. It is also of interest to evaluate other nonlinear anisotropic models, as well as a more fundamental treatment where the point-wise anisotropic response is calculated from orientations of fibrils at a finer scale. This can help tie in the parallel remodelling studies into this model.

But returning to our central theme—better represent the biochemistry—we see that the form of the source representing enzyme kinetics necessitates the introduction of at least one other species, a solute phase, s. The resulting and necessitated refinements motivate the next section.

3.2 Refining the formulation

In addition to being advected along with the fluid, the solute phase s can undergo transport relative to the fluid. To this end, an additional velocity split $\boldsymbol{V}^s = \widetilde{\boldsymbol{V}^s} + \boldsymbol{V}^f$, is introduced. The constitutive relation for the corresponding flux, now $\widetilde{\boldsymbol{M}^s}$, has a form similar to that defined for $\boldsymbol{M}^\iota$. Initial attempts at introducing this species resulted in an advection-diffusion equation that was unstable, and of a non-standard form. However, if the fluid is nearly incompressible, which is the case in reality, it can be shown that the balance of mass in the current configuration of the solute reduces to

$$\frac{\mathrm{d}\rho^s}{\mathrm{d}t} = \pi^s - \operatorname{div}\left(\widetilde{\boldsymbol{m}^s}\right) - \boldsymbol{m}^f \cdot \operatorname{grad}\left(\frac{\rho^s}{\rho^f}\right), \tag{3.3}$$

which has a standard advective-diffusion form, and thus it is amiable to documented stabilisation schemes, as seen in the next section.

Additionally, during the course of implementing the theory and solving initial-boundary value problems, potential refinements to the existing formulation have made themselves visible. Some of these changes include splitting permeability (stress-gradient driven) and diffusion (Fickean) mobilities in the constitutive relation for mass transport, and introducing a measure of saturation allowing greater control of the behaviour (for e.g., allowing swelling arising from fluid concentration increases to turn on only after the volume in question is fully saturated).

3.3 Numerical and computational aspects

As indicated in the preceding section, Eq. (3.3) can now be stabilised using standard methods such as the SUPG (see, for e.g., [Hughes et al., 1987]). The implementation has not been completed in the finite element code, but the unstable equation has been isolated and a `MATLAB` prototype implementation exists (see Figures 3.1 and 3.2 for a comparison between stabilised and non-stabilised forms for the simpler two-dimensional case) using ideas from [Hughes et al., 1987].

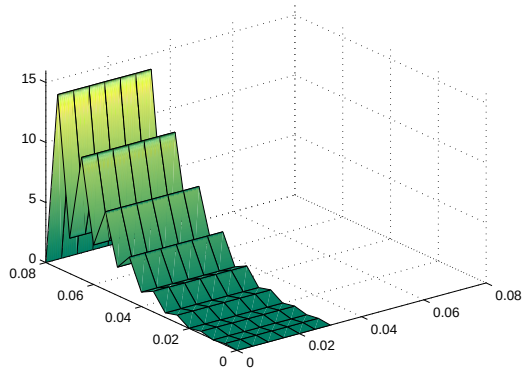

Figure 3.1: Advection-diffusion equation solution with stabilisation term turned off

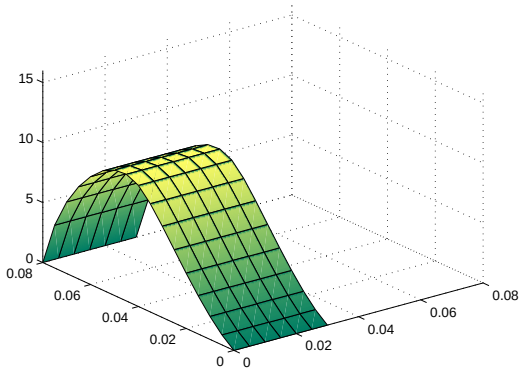

Figure 3.2: Advection-diffusion equation solution with stabilisation term turned on

A robust implementation of this is proposed to be incorporated into the finite element code. Furthermore, once the stability and rate of convergence of the algorithms for the individual differential equations are optimal, it is of interest to learn the tools to analyse and study the convergence of the overall coupled problem. Finally, the computational expense of the problem at hand is daunting. This issue needs to be circumvented by a suitable parallel implementation of `FEAP` or an externally interfaced solver.

3.4 Exploring applicability to other systems

This concluding section is not directly linked to the preceding sections.

While a substantial portion of effort in modelling the tendon system goes toward making ideal modelling choices to tailor the continuum field formulation to better reflect the tissue, the fundamental theory and physical principles employed are applicable to a large class of multi-species open systems. These other areas of application exist both in biology (injury mechanisms, wound healing, scarring, surgical repair, ...) as well as from other diverse fields (from porous soil mechanics, to diffusion of air through anisotropic rubber materials in automobile tyres).

With further enhancements to the theory and concurrent maturation of the resulting computational framework, it is of future interest to explore the applicability of the theory to these other classes of problems. If wound healing is of interest, for instance, as a first step, it could be thought of as a signalled growth localised to certain regions. This could conceivably be modelled using the existing framework by introducing an additional spatial variable which basically functions as a Boolean flag, switching off growth in regions and turning on growth where it is needed (near the site of the wound). Arriving at a small, but varied, class of relevant problems and applying the theory to those cases will result in further insight and additional inputs to the formulation.

Bibliography

[Ambrosi and Mollica, 2002] Ambrosi, D. and Mollica, F. (2002). On the mechanics of a growing tumor. *Int. J. Engr. Sci.*, 40:1297–1316.

[Armero, 1999] Armero, F. (1999). Formulation and finite element implementation of a multiplicative model of coupled poro-pplasticity at finite strains under fully-saturated conditions. *Comp. Methods in Applied Mech. Engrg.*, 171:205–241.

[Bischoff et al., 2002] Bischoff, J. E., Arruda, E. M., and Grosh, K. (2002). A microstructurally based orthotropic hyperelastic constitutive law. *J. Applied Mechanics*, 69:570–579.

[Calve et al., 2004] Calve, S., Dennis, R., Kosnik, P., Baar, K., Grosh, K., and Arruda, E. (2004). Engineering of functional tendon. *Tissue Engineering*, 10:755–761.

[Cowin and Hegedus, 1976] Cowin, S. C. and Hegedus, D. H. (1976). Bone remodeling I: A theory of adaptive elasticity. *Journal of Elasticity*, 6:313–325.

[Epstein and Maugin, 2000] Epstein, M. and Maugin, G. A. (2000). Thermomechanics of volumetric growth in uniform bodies. *International Journal of Plasticity*, 16:951–978.

[Garikipati et al., 2004] Garikipati, K., Arruda, E. M., Grosh, K., Narayanan, H., and Calve, S. (2004). A continuum treatment of growth in biological tissue: Mass transport coupled with mechanics. *Journal of Mechanics and Physics of Solids*, 52:1595–1625.

[Garikipati and Rao, 2001] Garikipati, K. and Rao, V. S. (2001). Recent advances in models for thermal oxidation of silicon. *Journal of Computational Physics*, 174:138–170.

[Harrigan and Hamilton, 1993] Harrigan, T. P. and Hamilton, J. J. (1993). Finite element simulation of adaptive bone remodelling: A stability criterion and a time stepping method. *Int. J. Numer. Methods Engrg.*, 36:837–854.

[Hughes et al., 1987] Hughes, T., Franca, L., and Mallet, M. (1987). A new finite element formulation for computational fluid dynamics: VII. Convergence analysis of the generalized SUPG formulation for linear time-dependent multidimensional advective-diffusive systems. *Comp. Methods in Applied Mech. Engrg.*, 63(1):97–112.

[Kuhl and Steinmann, 2003] Kuhl, E. and Steinmann, P. (2003). Theory and numerics of geometrically-nonlinear open system mechanics. *Int. J. Numer. Methods Engrg.*, 58:1593–1615.

[Lee, 1969] Lee, E. H. (1969). Elastic-Plastic Deformation at Finite Strains. *J. Applied Mechanics*, 36:1–6.

[Simo and Tarnow, 1992] Simo, J. C. and Tarnow, N. (1992). Exact energy-momentum conserving algorithms and symplectic schemes for nonlinear dynamics. *Comp. Methods in Applied Mech. Engrg.*, 100:63–116.

[Simo et al., 1985] Simo, J. C., Taylor, R. L., and Pister, K. S. (1985). Variational and projection methods for the volume constraint in finite deformation elasto-plasticity. *Comp. Methods in Applied Mech. Engrg.*, 51:177–208.

[Taber, 1995] Taber, L. A. (1995). Biomechanics of growth, remodelling and morphogenesis. *Applied Mechanics Reviews*, 48:487–545.

[Taber and Humphrey, 2001] Taber, L. A. and Humphrey, J. D. (2001). Stress-modulated growth, residual stress and vascular heterogeneity. *J. Bio. Mech. Engrg.*, 123:528–535.

[Taylor, 1999] Taylor, R. L. (1999). *FEAP - A Finite Element Analysis Program*. University of California at Berkeley, Berkeley, CA.

[Truesdell and Noll, 1965] Truesdell, C. and Noll, W. (1965). *The Non-linear Field Theories (Handbuch der Physik, band III)*. Springer, Berlin.